Pervasive Glucose Monitoring: A Non-invasive Approach Based on Near-Infrared Spectroscopy

Maria Valero(✉), Katherine Ingram, Anh Duong, and Valentina Nino

Kennesaw State University, Marietta, GA, USA
mvalero2@kennesaw.edu

Abstract. With more than 12% of Americans living with diabetes and more than 30% suffering from metabolic syndrome, the United States is facing the need for more technology for easy and non-invasive blood glucose monitoring. The current pervasive technologies can be leveraged as the foundation for new sensor devices and intelligent models to monitor and manage glucose. This paper presents an approach for monitoring glucose concentration with a pervasive device. The device capture and processes spectroscopy images of a body's extremity using a powerful machine learning model. The spectroscopy or spectral image is based on the theory of light intensity data from the spectrum. Using light absorption, the proposed sensor executes a model that permits glucose estimation. The procedure is noninvasive as no blood or needles are required. The device also pairs the information to a mobile application for real-time monitoring. Preliminary studies show an accuracy of 90.78% compared with traditional blood glucose estimation.

Keywords: Glucose Monitoring · Non-invasive Spectroscopy · Diabetes · Sensors · Machine Learning

1 Introduction

Pervasive computing has an essential role in healthcare applications [37]. Glucose monitoring, required for the successful management of diabetes, is enhanced by pervasive devices with the capacity of insitu computation [23]. Conventional glucose monitoring devices use an electrochemical method [13] to sample glucose concentration directly from blood or tissues. These require using a finger-prick to collect a droplet of blood or implanting a thin lancelet under the skin. The former provides a snapshot of the blood glucose concentration, while the latter provides continuous monitoring of glucose within the subcutaneous tissues. These minimally invasive methods involve inherent risks, including tissue damage and infection [49].

Non-invasive estimation of blood glucose concentrations with pervasive devices has emerged as an exciting alternative to collecting blood samples.

Supported by the University of Pennsylvania (NIA/NIH). Sub-Award # 587764.

D. Salvi et al. (Eds.): PH 2023, LNICST 572, pp. 274–289, 2024.
https://doi.org/10.1007/978-3-031-59717-6_19

However, current non-invasive technologies for estimating blood glucose are inaccurate, complicated to use, and/or expensive. methods using *Surface Plasmon Resonance (SPR)* [30] require a metal surface, typically gold, and is dependent on the refractive index of the medium. In addition, this method is sensitive to motion, requires a long calibration process, and involves carrying a large, inconvenient device [58]. Methods based on *fluorescence* [16] are more robust to variations in glucose concentration but are susceptible to interference from changes in pH and oxygen levels and carry a high risk of infection from contamination within the biological media [58]. *Optical Polarimetry (OP)* uses light transmitted through the retina of the eye to determine blood glucose concentration [34,44]. This technology benefits from good resolution, however the method is prone to interference from temperature changes, motion, and optically active compounds [58]. *Near-infrared Spectroscopy* [2] is becoming increasingly utilized as an alternative method to estimate blood glucose for its relatively low cost, minimal sample preparation, and its robustness to interference from substances, such as glass or plastic [58].

In this paper, we compare current methods of glucose estimation and describe our approach, including a detailed evaluation of a novel, non-invasive approach to pervasively monitor blood glucose using near-infrared spectroscopy. The glucose sensor is a small, intelligent device that can be fitted to a finger or ear. It is paired with a mobile application and smart voice assistant to deliver real-time blood glucose results. Our work contributes:

- Real-time non-invasive blood glucose monitoring based on near-infrared spectroscopy and machine learning.
- Rapid glucose detection suitable for pervasive devices and executed on a single-board computer.
- A device with 90.78% accuracy that has been validated against a popular commercial-grade glucometer in a racially-diverse population.

2 Related Works

Diabetes and metabolic disease are considered a silent epidemic in the United States [46]. Monitoring blood glucose is critical for the successful management of diabetes, though it involves either extracting blood several times per day or implanting subcutaneous needles. Both of these can be invasive, uncomfortable, and associated with risk of infection. Non-invasive methods to estimate blood glucose have been proposed and are summarized in Fig. 1.

Noninvasive technology for monitoring blood glucose has limitations, and each approach carries a unique set of challenges. Electrical approaches [19,35,47,54] are overly sensitive to environment temperature, causing serious errors in the detection of the glucose level [22,58]. Thermal approaches [8,12,52,53] are susceptible to interference by skin conditions making the sensors very sensitive to sweat, leading to inaccuracies. This technology integration time is long and expensive, making it a poor choice for disadvantaged population [58]. Nanotechnology approaches [5,9,28,41], introduce issues with potential toxicity in

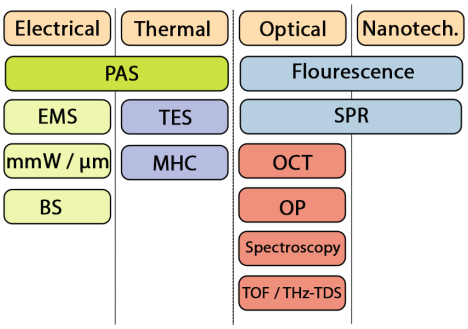

Fig. 1. Non-invasive approaches for blood glucose estimation. Photoacustic Spectroscopy (PAS), Electromagnetic Sensing (EMS), mmW-milimeter wave (mmW/µm), Bioimpedance Spectroscopy (BP), Termal Spectroscopy (TES), Metabolic Heat Conformation (MHC), Optical Coherence Tomography (OCT), Optical Polarimetry (OP), Time of Flight (TOF), Terahertz Time Domain Spectroscopy (THzTDS), Surface Plasmon Resonance (SPR).

addition to poor lifespan, poor photostability, and poor accessibility due to the need for expensive materials [58].

Optical technologies are becoming increasingly adopted for use in noninvasive glucose estimation in response to these challenges, though they are not completely free of limitations. *Mid-Infrared Spectroscopy* [15,31,32] is a vibrational spectroscopy technique that has provided the capacity to obtain signals from skin regions. However, this approach is expensive and has poor penetration in deep skin, which limits its effectiveness in glucose estimation [58]. *Raman Spectroscopy* [33,38,59] provides a way to measure molecular composition through inelastic scattering, but it is prone to interference by other molecules such as hemoglobin and has a lengthy collection time [58]. *Far-Infrared Spectroscopy* [53] has less scattering than Raman approaches, but has strong water absorption that makes extremely difficult the identification of molecules in the sample [58]; the *Time of Flight* and *Terahertz Time-Domain Spectroscopy* [11,20] uses short and ultrashort laser pulses to measure the travel time of the reflected signals, but have long measurement time and low spatial and depth resolution [58].

Finally, the *Near-Infrared Spectroscopy (NIR)*, which relies on the absorption and scattering of wavelengths, has the advantage of being low cost, the signal intensity is directly proportional to the concentration of the analyte, requires minimal sample preparation, and works in the presence of interfering substances such glass and plastic [58]. Monte-Moreno et. al [36] used this method to estimate blood sugar, obtaining a Clarke error grid placed 87.7% of points in zone A, 10.3% in zone B, and 1.9% in zone C. Yamakoshi et al. [60] also use NIR for estimating glucose, obtaining a Clarke error grid placed 90.05% of points in zone A, and 9.95% in zone B. Also, Alarcon-Paredes et al. [3] used this technology to estimate blood sugar with a Clarke error placed 90.32% of points in zone A, and 9.68% in zone B. For information about Clarke error and zones, refer to Sect. 6.4.

While previous studies exhibit promising results, our proposed work is novel because (1) we incorporate a machine learning statistical approach that has not been used before for glucose estimation; (2) we develop a light method that can be run in pervasive devices and present results in real-time, and (3) we exhibit better results with more rigorous evaluation, including Parkes error grid [40], a more robust method to evaluate glucose estimation devices.

3 Principles of Near-Infrared Spectroscopy for Glucose Estimation

Near-infrared spectroscopy (NIR) illuminates the target tissue with a near-infrared light to visualize the organic composition of the material or tissue of interest [56]. NIR light waves contain a broad spectrum of wavelengths and frequencies, which are then absorbed, transmitted, reflected, or scattered by the sample of interest [42]. In our model, a polychromatic light source (Light Emitting Diode (LED)) is radiated through the sample. A diffraction grating then splits the transmitted radiation into its constituent wavelengths to a camera (sensor) and the images are analyzed by a computer board (detector). Figure 2 illustrates this absorption mode. Our prototype uses image capture via camera for its superior speed, replicability, and accessibility, in comparison to other forms of spectroscopy measurement, such as light intensity and Photoplethysmography (PPG) signals.

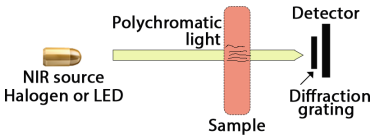

Fig. 2. Foundation of Near-Infrared Spectroscopy.

Our approach is based on the Beer-Lambert law of absorption that is shown in Eq. 1 [48].

$$I = I_0 10^{(-l.\epsilon.c)} = I_0 10^{(-l.\mu_a)}, \tag{1}$$

where I_0 is the initial light intensity (W/cm^2), I is the intensity of the ith at any depth within the absorption medium in W/cm^2, l is the absorption depth within the medium in cm, ϵ is the molar extinction coefficient in $L/(\text{mmol cm})$, and c is the concentration of absorbing molecules in mmol/L. The product of ϵ and c is proportional to the absorption coefficient (μ_a).

The concentration of absorbing molecules is based on the above equation. However, the effect of other blood components and absorbing tissue components affect the amount of light absorbed. As a result, the total absorption coefficient is the summation of the absorption coefficients of all the absorbing components [26]. Then, to minimize the absorption due to all the other components, the wavelength of the light source should be chosen so that the light source is highly absorbed by glucose and is mostly transparent to blood and tissue components.

4 Approach Overview

Our prototype uses a clip attached to a finger or other accessible extremity and irradiates a NIR laser light of 650 nm and 5 mW voltage. On the other side of the clip, a Raspberry PI camera captures the diffraction grating images. A small computer board extracts data from the images and applies a machine learning model to generate estimates of blood glucose concentration. The data is saved to an InfluxDB time-series database [24] for continuous data collection. Figure 3(a) illustrates the prototype and approach.

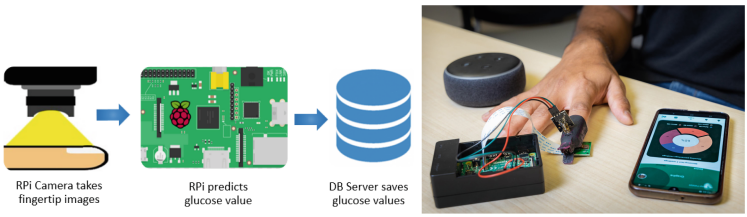

(a) (b)

Fig. 3. (a) General overview of the proposed approach. (b) Prototype structure and external communication with other devices of the proposed approach.

The associated mobile application displays real-time results from the database. The database is also accessible via AMAZON ALEXA, which will reply to commands related to the current blood glucose concentration and recent history of blood glucose patterns when commanded. Figure 3(b) depicts the prototype compared with other pervasive devices for glucose estimation.

5 System Design

5.1 Data Gathering and Cleaning

Images are collected using a KY-008 laser transmitter with a 5 mW voltage and a wavelength of 650 nm. The size of the laser is 24×15 mm/0.94×0.59 inch(L*W). A 640×480 resolution was selected to preserve small details without sacrificing computing time and resources. The standard RGB (red, green, and blue) color format was used. An average of 15 measures for each sample was used to minimize the influence of random errors such as the noise of the spectrometer and variations in humidity within the laboratory. A set of 4 fingertip images is shown in Fig. 4.

5.2 Features Extraction

Each image is analyzed by three color channels (red, green, and blue) and also in grayscale. For each channel, the image is first converted into numerical tensors with 3-dimensional matrices. The tensors are then converted into

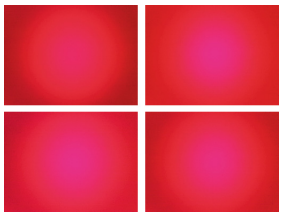

Fig. 4. Example of spectroscopy images collected from a finger at 8 s (top left), 16 s (top right), 24 s (bottom left), and 32 s (bottom right) after comparison blood draw.

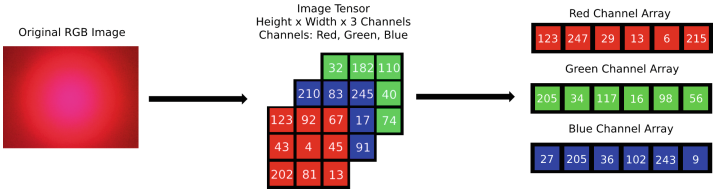

Fig. 5. Demonstration of Measurement Dataset Creation

a one-dimensional array and pixel statistics are calculated including center of mass, minimum, maximum, mean, median, standard deviation, and variance, as depicted in Fig. 5.

Values for each channel were compiled into the same dataset with the comparison blood glucose value and repeated for each image. The resulting "Measurement Dataset" consisted of seven measures from each of the four channels plus one measure of the blood glucose, for a total of 29 distinct measures. Next, the 29 measures from the image are merged with the intensity values of the image. The intensity values are calculated as follows: for each possible value of red, green, and blue (0–255), the number of pixels with that same value in an image can be counted and recorded in a histogram [21]. Through this process, a histogram with RGB values on the x-axis (256 possible values for red, green, and blue) and the number of pixels on the y-axis can be created, as shown in Fig. 6.

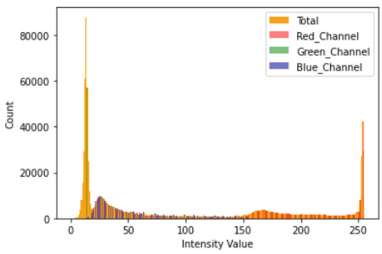

Fig. 6. Histogram of RGB Intensity Values in an Image.

The merge of the 29 measures from each of the four channels and the intensities estimated via the image's histogram, produce four new datasets: "Red-

Measurement", "Green-Measurement", "Blue-Measurement", and "RGB- Measurement". The first three new datasets contained 285 features: 256 for the pixel intensities, 28 for the measurement features, and one for the blood glucose value. The last new dataset contained 797 features: 256 for each color channel, 28 measurement features, and one for the blood glucose value.

5.3 Model Selection

In our previous works [55], we use a Convolutional Neural Network (CNN)to estimate glucose from spectroscopy images reaching only 72% accuracy. Then, we decide to compare multiple machine learning models to determine the best one for our type of images and data. We selected the AdaBoost classifier trained with KNN for its accuracy and its ability to adapt to the limited computing resources of the computer board [51], as described in Sect. 6. It was evaluated against other popular classifiers, including Random Forest [17], Elastic Net [57], Support Vector Machine [43], Bayesian Ridge [45], and XGBoost [7] and the results are reported in [27].

AdaBoost is a meta-estimator regressor that fits multiple copies of the model in layers onto the original dataset using adjusted weights of instances based on the error of the current prediction [1]. The layers are versions of the same model that tackle different sections of the training data, which results in reduced error overall. Due to the large number of varying estimators created by AdaBoost, the model is much less prone to overfitting than other models.

In contrast, KNN classifies a data point based on its nearest neighbors in the graph. It is a non-parametric supervised learning method used for classification and regression [29]. The regression algorithm uses the average values from a specified number of the nearest data and does not make assumptions. Therefore the algorithm handles outliers and minimizes error better in many cases than other algorithms, such as decision trees and linear regression. This model was selected for our approach due to its novel approach to ensemble learning, high training speed, and high performance.

AdaBoost is known as an effective method for improving the performance of base classifiers [10], though previous studies have shown that it is prone to overfitting [18]. To accommodate this limitation, we employ the KNN algorithm for its simplistic method of pattern classification. When KNN is combined with prior knowledge, it often yields competitive results. In our model, we combine AdaBoost and KNN as complementary strategies, employing AdaBoost for training the data and adding a weighted KNN algorithm on the classifiers produced by AdaBoost to generate accurate results.

6 Experiments

6.1 Experiment Ethics

The study was approved by the Institutional Review Board at Kennesaw State University (IRB-FY22-318). All participants provided written consent before participating.

6.2 Data Collection

A racially-diverse cohort of 43 individuals (23F/20M) between 18 and 65 years old participated in this study. Only 1 participant had diabetes, while the rest were normoglycemic. Participants were instructed to fast for at least four hours prior to testing and to remove any dark nail polish to minimize its potential impact on light absorption.

Glucose data were collected in two rounds: one at baseline and the other 1 h later, after eating a self-selected snack containing carbohydrates to modify glucose levels. Each round provided a set of 15 images collected from the finger and a finger prick blood draw to estimate blood glucose from the FORA 6 Connect BG50 glucometer per manufacturer instructions. After data cleaning, the final dataset consisted of 1128 sample images. Data collection and the glucometer are depicted in Fig. 7.

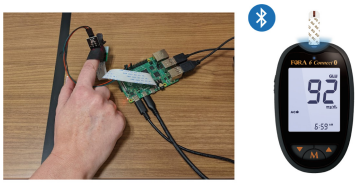

(a) (b)

Fig. 7. (a) Example of data collection. (b) Glucometer used for comparison purposes.

6.3 Training of the Model

Data were divided into subsets for training (75%) and evaluation (25%). The training data is used to train the models to identify patterns, while the evaluation data is used to evaluate the predictive quality of the trained model.

6.4 Evaluation Rigor

Error Grids. Both Clarke and Parkes error grids were used to test the accuracy of our method in comparison to estimates from our referent device, the FORA 6 Connect glucometer [6]. For the Clarke Error Grid, data collected from the two devices are plotted and compared according to the degree of risk that an erroneous measurement would represent [58]. The degree of risk is divided into five regions, as depicted in Fig. 8. RData in Region A is considered "clinically accurate", while those in Region B are considered "clinically acceptable". Data found in Regions C, D, and E are considered clinically inaccurate and dangerous due to the potential for misdiagnosis [14]. The Parkes error grid similarly uses five risk levels for comparative analysis [39] and represents a new set of innovative error grids based on the proficiency of a big group of medical experts.

ISO 15197 Standard. The International Standards Organization (ISO) defines specifications for the reliability of medical devices, including glucometers [25]. The ISO standard (2013) requires that 95% of the results are within a glucose concentration of pm 15 mg/dL, compared with the reference method, for concentrations less than 100 mg/dL, or pm15% of zones A and B of the Parkes (Consensus) Error Grid [50].

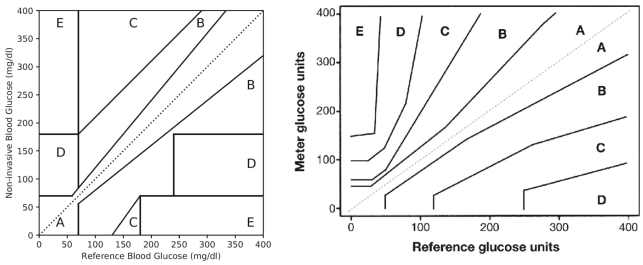

(a) (b)

Fig. 8. Error grids (a) Clarke. (b) Parkes.

6.5 Data Analysis

The model performance was compared using the Mean Average Error (MAE) and the percent of data that falls into Zone A of the Clarke Error Grid, indicating "clinically accurate". Mean Average Error (MAE) and Root Mean Square Error (RMSE) were calculated. Models were further trained, tuned, and tested against the testing data. Findings are displayed in Table 1.

Table 1. Model Testing Results from Measurement Datasets - MAE and Zone A percentages from Clarke error grid analysis

	RM	GM	BM	GBM
Random Forest	12.85–87.23%	12.63–86.52%	13.91–85.82%	12.74–88.65%
Elastic Net	15.68–84.04%	16.89–85.11%	15.55–81.56%	14.41–83.69%
KNeighbors	9.55–90.78%	14.3–86.17%	15.81–84.4%	12.43–87.59%
Support Vector	14.3–87.94%	15.02–89.01%	14.58–87.23%	13.28–87.94%
Bayesian Ridge	15.52–84.04%	17.43–85.46%	15.52–82.62%	14.3–83.33%
XGBoost	13.03–86.88%	12.86–88.3%	13.6–86.52%	12.89–87.59%
AdaBoost	9.4–90.78%	12.74–86.88%	13.41–87.59%	13.18–86.52%

AdaBoost with KNeighbors trained on the Red-Measurement dataset provided the most accurate blood glucose estimates among all of the dataset models

tested (MAE, 9.4 mg/dl; RMSE, 16.72 mg/dl). As shown in Fig. 9(a), all data were located in Zones A and B, with 90.72% of the measures in Zone A ("clinically accurate") and 9.22% in Zone B ("clinically acceptable"). No values were outside of these categories.

The Parkes Error Grid, was also used to evaluate our model. As shown in Fig. 9(b), 87.2% of the values were in Zone A, while 11.7% were in Zone B. Two measures (1.1%) narrowly extended into Zone C, and were classified as "clinically inaccurate - likely to affect the clinical outcome".

We used the Parkes Error Grid to further evaluate our model. Figure 9(b) shows the results based on this error. In this case, 87.2% of the values fell into Zone A or "clinically accurate", 11.7% fell in Zone B or "clinically acceptable", and 1.1% fell in Zone C or "clinically inaccurate – likely to affect clinical outcome".

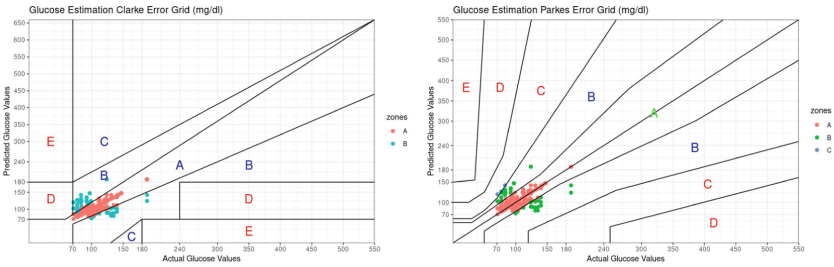

(a) (b)

Fig. 9. (a) Clarke Error Grid. (b) Parkes Error Grid.

Table 2. Sample comparison of results of the proposed approach and the ground truth

	Demographics			Glucometer Readings		Proposed Approach Readings		Errors (mg/dL)		
	Age	Gender	Race	First	Second	First	Second	Error 1	Error 2	Av. Error
1	43	Female	White	83	85	83	88	0.0	3.53	1.77
2	21	Male	Black	113	120	113	115	0.0	4.17	2.09
3	24	Female	White	98	98	99	99	1.02	1.02	1.02
4	33	Female	Latino	92	95	93	96	1.09	1.05	1.07
5	24	Male	Latino	100	124	96	125	4.0	0.81	2.41
6	18	Female	Asian	82	84	83	87	1.22	3.19	2.21
7	18	Female	Black	95	100	98	94	3.16	6.0	4.58
8	31	Female	White	108	131	105	123	2.78	6.11	4.45
9	41	Male	Latino	84	105	89	102	5.95	2.86	4.41
10	24	Female	Latino	87	96	89	95	2.3	1.04	1.67
11	29	Female	Black	80	102	82	101	2.5	0.98	1.74
12	39	Male	Asian	80	102	80	102	2.5	0.98	1.74
13	27	Female	White	80	106	84	105	5.0	0.94	2.97
14	29	Male	Asian	83	101	85	99	2.41	1.98	2.2
15	28	Male	Asian	87	140	86	133	1.15	5.0	3.08
...	...	...	...	...	...	...	...	...	...	...

6.6 Discussion on Accuracy

A comparison between glucose estimates from our model and from the FORA6 Connect for 15 individual participants is shown in Table 2. The average deviation between the actual value and the estimated value is within ±1.02 mg/dL and ±4.5 mg/dL. Our prototype and model meet the ISO 15197 standard requiring ±15% of data to be within Zones A and B.

We further compared the accuracy of our approach with published findings of other noninvasive approaches using the Clark Error method only. Figure 10 illustrates our accuracy compared with these approaches [36,60], and [3]. None of these studies had Parkes Error grid data available, and therefore we cannot make comparisons with these data. Our findings indicate that the accuracy of our approach is as strong as, or superior to, other approaches that have been introduced.

6.7 Discussion on Demographics

The accuracy of the device was tested across a diverse range of races and ethnicity, age, and gender. Mean glucose estimates were similar in males and females (Fig. 11(a)).

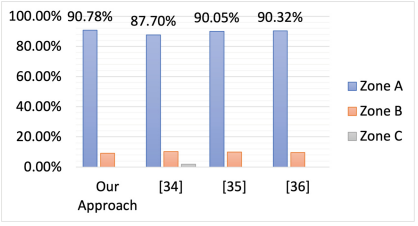

Fig. 10. Clarke error accuracy comparison with other research approaches.

No significant difference in average error was observed in mean glucose concentration when data was stratified and analyzed by mean age (30 years) or sex, as shown in Fig. 11(b) We found no significant difference in the average error between both groups.

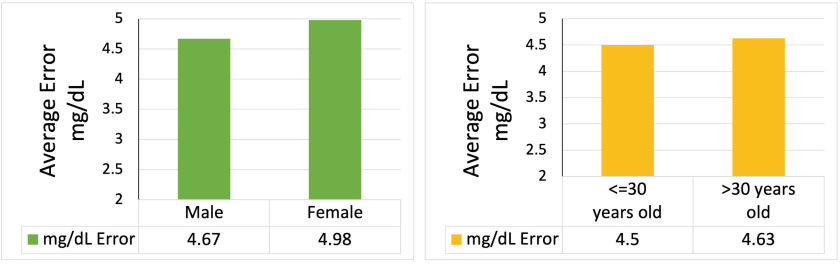

(a) (b)

Fig. 11. Comparison of average error in mg/dL based on (a) gender, (b) age.

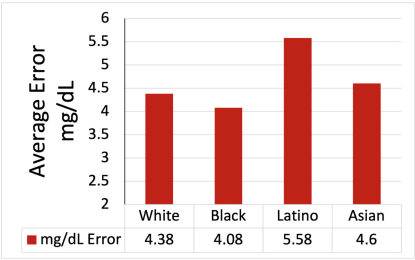

Fig. 12. Comparison of average error in mg/dL based on race.

Finally, glucose estimates were compared by differences in skin pigmentation to test our hypothesis that darker skin tones would yield less accurate results than lighter tones. In Fig. 12 the results of the average error in terms of race are presented. Glucose estimates for Latino and Asian participants were less accurate than those for the other participants, while estimates for black individuals were more accurate than the white participants. These findings suggest that measures taken on lighter skin tones are less accurate than those taken on darker skin tones, counter to our original hypothesis. More research is needed to study the effect of skin pigmentation on the accuracy of these models.

7 Limitations

The following limitations were identified. We have created a strategy to overcome these issues in our future work:

- External Factors: Depending on the radiation used, a viable noninvasive optical sensor must consider skin pigmentation, surface roughness, skin thickness, breathing artifacts, blood flow, body movements, and ambient temperature [4]. We plan to address all these factors in future enhancements of the model. Currently, we are not analyzing the impact of these factors, but our vision is to add some of these features into account to understand the reliability of the prototype and the technique.
- Prototype enclosure design: Our prototype design is in development with the goal of maximizing usability.

8 Conclusion

In this paper, we presented a non-invasive pervasive glucose monitoring approach for diabetes management that is based on near-infrared spectroscopy and machine learning techniques that leverage sensor device computation power. This approach uses images collected through the skin on a finger or ear and does not require blood samples. After testing several machine learning models, we have determined that AdaBoost trained with KNeighbors is the best model for

estimating blood glucose from images collected by spectroscopy. Furthermore, the red channel provides the best color intensity data for training the model. Our final model had a 90.78% clinical accuracy rate based on the Clark Error Grid. and had 87.2% clinical accuracy using the Parkes Error Grid. Our approach performed as well or better than other published approaches. The ability to connect our prototype with a mobile application and a voice assistant makes this approach an attractive alternative to current methods of glucose monitoring and a potentially life-changing technology for people with diabetes.

Acknowledgments. Research reported in this publication was supported by the National Institute On Aging of the National Institutes of Health under Award Number P30AG073105. The content is solely the responsibility of the authors and does not necessarily represent the official views of the National Institutes of Health.

Conflict of Interest. All authors declare that they have no conflicts of interest.

References

1. Sklearn.ensemble.adaboostregressor. https://scikit-learn.org
2. Agelet, L.E., Hurburgh, C.R., Jr.: A tutorial on near infrared spectroscopy and its calibration. Crit. Rev. Anal. Chem. **40**(4), 246–260 (2010)
3. Alarcón-Paredes, A., Francisco-García, V., Guzmán-Guzmán, I.P., Cantillo-Negrete, J., Cuevas-Valencia, R.E., Alonso-Silverio, G.A.: An iot-based non-invasive glucose level monitoring system using raspberry pi. Appl. Sci. **9**(15), 3046 (2019)
4. do Amaral, C.E.F., Wolf, B.: Current development in non-invasive glucose monitoring. Med. Eng. Phys. **30**(5), 541–549 (2008)
5. Barone, P.W., Strano, M.S.: Single walled carbon nanotubes as reporters for the optical detection of glucose. J. Diabetes Sci. Technol. **3**(2), 242–252 (2009)
6. Boren, S.A., Clarke, W.L.: Analytical and clinical performance of blood glucose monitors. J. Diabetes Sci. Technol. **4**(1), 84–97 (2010)
7. Brownlee, J.: Xgboost for regression (Mar 2021). https://machinelearningmastery.com/xgboost-for-regression/
8. Buchert, J.M.: Thermal emission spectroscopy as a tool for noninvasive blood glucose measurements. In: Optical Security and Safety, vol. 5566, pp. 100–111. SPIE (2004)
9. Chen, L., Hwang, E., Zhang, J.: Fluorescent nanobiosensors for sensing glucose. Sensors **18**(5), 1440 (2018)
10. Chen, Y., Dou, P., Yang, X.: Improving land use/cover classification with a multiple classifier system using adaboost integration technique. Remote Sens. **9**(10), 1055 (2017)
11. Cherkasova, O., Nazarov, M., Shkurinov, A.: Noninvasive blood glucose monitoring in the terahertz frequency range. Opt. Quant. Electron. **48**(3), 1–12 (2016)
12. Cho, O.K., Kim, Y.O., Mitsumaki, H., Kuwa, K.: Noninvasive measurement of glucose by metabolic heat conformation method. Clin. Chem. **50**(10), 1894–1898 (2004)
13. Clark, L.C., Jr., Lyons, C.: Electrode systems for continuous monitoring in cardiovascular surgery. Ann. N. Y. Acad. Sci. **102**(1), 29–45 (1962)

14. Clarke, W.L., Cox, D., Gonder-Frederick, L.A., Carter, W., Pohl, S.L.: Evaluating clinical accuracy of systems for self-monitoring of blood glucose. Diabetes Care **10**(5), 622–628 (1987)
15. Coates, J.: Vibrational spectroscopy: instrumentation for infrared and raman spectroscopy. Appl. Spectrosc. Rev. **33**(4), 267–425 (1998)
16. DiCesare, N., Lakowicz, J.R.: Evaluation of two synthetic glucose probes for fluorescence-lifetime-based sensing. Anal. Biochem. **294**(2), 154–160 (2001)
17. Donges, N., Contributor, E., entrepreneur, N.a.: Random forest algorithm: a complete guide. https://builtin.com/data-science/random-forest-algorithm
18. Gao, Y., Pan, J.y., Gao, F.: Improved boosting algorithm through weighted k-nearest neighbors classifier. In: 2010 3rd International Conference on Computer Science and Information Technology, vol. 6, pp. 36–40. IEEE (2010)
19. Gourzi, M., et al.: Non-invasive glycaemia blood measurements by electromagnetic sensor: study in static and dynamic blood circulation. J. Med. Eng. Technol. **29**(1), 22–26 (2005)
20. Gusev, S., et al.: Application of terahertz pulsed spectroscopy for the development of non-invasive glucose measuring method. In: 2017 Progress In Electromagnetics Research Symposium-Spring (PIERS), pp. 3229–3232. IEEE (2017)
21. Guzmán-Guzmán, I.P., Cuevas-Valencia, R.E.: An iot-based non-invasive glucose level monitoring system using raspberry pi (Jul 2019). https://www.mdpi.com/2076-3417/9/15/3046/htm
22. Haller, M.J., Shuster, J.J., Schatz, D., Melker, R.J.: Adverse impact of temperature and humidity on blood glucose monitoring reliability: a pilot study. Diabetes Technol. Therapeut. **9**(1), 1–9 (2007)
23. Hartz, J., Yingling, L., Powell-Wiley, T.M.: Use of mobile health technology in the prevention and management of diabetes mellitus. Curr. Cardiol. Rep. **18**(12), 1–11 (2016)
24. Influxdata Inc: InfluxDB (2019). https://www.influxdata.com/
25. International Organization for Standarization (ISO). https://www.iso.org
26. Jacques, S.L.: Optical properties of biological tissues: a review. Phys. Med. Biol. **58**(11), R37 (2013)
27. Kazi, T., Ponakaladinne, K., Valero, M., Zhao, L., Shahriar, H., Ingram, K.I.: Comparative study of machine learning methods on spectroscopy images for blood glucose estimation. In: for Innovation, E.A. (ed.) EAI PervasiveHealth 2022 - 16th EAI International Conference on Pervasive Computing Technologies for Healthcare, Tessaloniki, Greece (December 2022)
28. Klonoff, D.C.: Overview of fluorescence glucose sensing: a technology with a bright future. J. Diabetes Sci. Technol. **6**(6), 1242–1250 (2012)
29. Kramer, O.: K-nearest neighbors. In: Dimensionality Reduction with Unsupervised Nearest Neighbors, pp. 13–23. Springer (2013). https://doi.org/10.1007/978-3-031-02363-7_6
30. Li, D., et al.: Glucose measurement using surface plasmon resonance sensor with affinity based surface modification by borate polymer. In: 2015 Transducers-2015 18th International Conference on Solid-State Sensors, Actuators and Microsystems (TRANSDUCERS), pp. 1569–1572. IEEE (2015)
31. Liakat, S., Bors, K.A., Huang, T.Y., Michel, A.P., Zanghi, E., Gmachl, C.F.: In vitro measurements of physiological glucose concentrations in biological fluids using mid-infrared light. Biomed. Opt. Express **4**(7), 1083–1090 (2013)
32. Liakat, S., Bors, K.A., Xu, L., Woods, C.M., Doyle, J., Gmachl, C.F.: Noninvasive in vivo glucose sensing on human subjects using mid-infrared light. Biomed. Opt. Express **5**(7), 2397–2404 (2014)

33. Lundsgaard-Nielsen, S.M., Pors, A., Banke, S.O., Henriksen, J.E., Hepp, D.K., Weber, A.: Critical-depth raman spectroscopy enables home-use non-invasive glucose monitoring. PLoS ONE **13**(5), e0197134 (2018)
34. Malik, B.H., Coté, G.L.: Real-time, closed-loop dual-wavelength optical polarimetry for glucose monitoring. J. Biomed. Opt. **15**(1), 017002 (2010)
35. Melikyan, H., et al.: Non-invasive in vitro sensing of d-glucose in pig blood. Med. Eng. Phys. **34**(3), 299–304 (2012)
36. Monte-Moreno, E.: Non-invasive estimate of blood glucose and blood pressure from a photoplethysmograph by means of machine learning techniques. Artif. Intell. Med. **53**(2), 127–138 (2011)
37. Orwat, C., Graefe, A., Faulwasser, T.: Towards pervasive computing in health care-a literature review. BMC Med. Inform. Decis. Mak. **8**(1), 1–18 (2008)
38. Pandey, R., et al.: Noninvasive monitoring of blood glucose with raman spectroscopy. Acc. Chem. Res. **50**(2), 264–272 (2017)
39. Parkes, J.L., Slatin, S.L., Pardo, S., Ginsberg, B.H.: A new consensus error grid to evaluate the clinical significance of inaccuracies in the measurement of blood glucose. Diabetes Care **23**(8), 1143–1148 (2000)
40. Pfützner, A., Klonoff, D.C., Pardo, S., Parkes, J.L.: Technical aspects of the parkes error grid. J. Diabetes Sci. Technol. **7**(5), 1275–1281 (2013)
41. Pickup, J.C., Hussain, F., Evans, N.D., Rolinski, O.J., Birch, D.J.: Fluorescence-based glucose sensors. Biosens. Bioelectron. **20**(12), 2555–2565 (2005)
42. Prieto, N., Pawluczyk, O., Dugan, M.E.R., Aalhus, J.L.: A review of the principles and applications of near-infrared spectroscopy to characterize meat, fat, and meat products. Appl. Spectrosc. **71**(7), 1403–1426 (2017)
43. Raj, A.: Unlocking the true power of support vector regression (Oct 2020)
44. Rawer, R., Stork, W., Kreiner, C.F.: Non-invasive polarimetric measurement of glucose concentration in the anterior chamber of the eye. Graefes Arch. Clin. Exp. Ophthalmol. **242**(12), 1017–1023 (2004)
45. Rothman, A.: The bayesian paradigm & ridge regression (Dec 2020). https://towardsdatascience.com
46. Sherling, D.H., Perumareddi, P., Hennekens, C.H.: Metabolic syndrome: clinical and policy implications of the new silent killer. J. Cardiovasc. Pharmacol. Ther. **22**(4), 365–367 (2017)
47. Siegel, P.H., Tang, A., Virbila, G., Kim, Y., Chang, M.F., Pikov, V.: Compact non-invasive millimeter-wave glucose sensor. In: 2015 40th International Conference on Infrared, Millimeter, and Terahertz waves (IRMMW-THz), pp. 1–3. IEEE (2015)
48. Singh, K., Sandhu, G., Lark, B., Sud, S.: Molar extinction coefficients of some carbohydrates in aqueous solutions. Pramana **58**(3), 521–528 (2002)
49. So, C.F., Choi, K.S., Wong, T.K., Chung, J.W.: Recent advances in noninvasive glucose monitoring. Med. Dev. (Auckland, NZ) **5**, 45 (2012)
50. for Standardization, I.O.: In vitro diagnostic test systems: requirements for blood-glucose monitoring systems for self-testing in managing diabetes mellitus. ISO (2003)
51. Suja, P., Tripathi, S., et al.: Real-time emotion recognition from facial images using raspberry pi ii. In: 2016 3rd International Conference on Signal Processing and Integrated Networks (SPIN), pp. 666–670. IEEE (2016)
52. Tanaka, Y., Tajima, T., Seyama, M.: Differential photoacoustic spectroscopy with continuous wave lasers for non-invasive blood glucose monitoring. In: Photons Plus Ultrasound: Imaging and Sensing 2018, vol. 10494, pp. 494–498. SPIE (2018)
53. Tang, F., Wang, X., Wang, D., Li, J.: Non-invasive glucose measurement by use of metabolic heat conformation method. Sensors **8**(5), 3335–3344 (2008)

54. Tura, A., Sbrignadello, S., Cianciavicchia, D., Pacini, G., Ravazzani, P.: A low frequency electromagnetic sensor for indirect measurement of glucose concentration: in vitro experiments in different conductive solutions. Sensors **10**(6), 5346–5358 (2010)
55. Valero, M., et al.: Development of a noninvasive blood glucose monitoring system prototype: Pilot study. JMIR Formative Res. **6**(8), e38664 (2022)
56. Van Kempen, T.: Infrared technology in animal production. Worlds Poult. Sci. J. **57**(1), 29–48 (2001)
57. Verma, Y.: Hands-on tutorial on elasticnet regression (Aug 2021). https://analyticsindiamag.com/hands-on-tutorial-on-elasticnet-regression/
58. Villena Gonzales, W., Mobashsher, A.T., Abbosh, A.: The progress of glucose monitoring-a review of invasive to minimally and non-invasive techniques, devices and sensors. Sensors **19**(4), 800 (2019)
59. Xu, Y., et al.: Raman measurement of glucose in bioreactor materials. In: Biomedical Sensing, Imaging, and Tracking Technologies Ii, vol. 2976, pp. 10–19. SPIE (1997)
60. Yamakoshi, K.i., Yamakoshi, Y.: Pulse glucometry: a new approach for noninvasive blood glucose measurement using instantaneous differential near-infrared spectrophotometry. J. Biomed. Opt. **11**(5), 054028 (2006)